Spectral statistics and dynamics of Lévy matrices

Mariela Araujo,[1] Ernesto Medina,[2,*] and Eduardo Aponte[3]
[1]*PDVSA Intevep, Apartado 76343, Caracas 1070A, Venezuela*
[2]*Laboratorio de Física Estadística de Sistemas Desordenados, Centro de Física, IVIC, Apartado 21827, Caracas 1020-A, Venezuela*
[3]*Laboratorio de Física Computacional, Universidad Nacional Experimental Politécnica, Torre Domus 14-B, Caracas, Venezuela*
(Received 10 December 1998; revised manuscript received 25 May 1999)

We study the spectral statistics and dynamics of a random matrix model where matrix elements are taken from power-law tailed distributions. Such distributions, labeled by a parameter μ, converge on the Lévy basin, giving the matrix model the label ''Lévy matrix'' [P. Cizeau and J. P. Bouchaud, Phys. Rev. E **50**, 1810 (1994)]. Such matrices are interesting because their properties go beyond the Gaussian universality class and they model many physically relevant systems such as spin glasses with dipolar or Ruderman-Kittel-Kasuya-Yosida interactions, electronic systems with power-law decaying interactions, and the spectral behavior at the metal insulator transition. Regarding the density of states we extend previous work to reveal the sparse matrix limit as $\mu \to 0$. Furthermore, we find for 2×2 Lévy matrices that geometrical level repulsion is not affected by the distribution's broadness. Nevertheless, essential singularities particular to Lévy distributions for small arguments break geometrical repulsion and make it μ dependent. Level dynamics as a function of a symmetry breaking parameter gives new insight into the phases found by Cizeau and Bouchaud (CB). We map the phase diagram drawn qualitatively by CB by using the Δ_3 statistic. Finally we compute the conductance of each phase by using the Thouless formula, and find that the mixed phase separating conducting and insulating phases has a unique character. [S1063-651X(99)00910-1]

PACS number(s): 02.50.−r, 05.45.Mt, 72.15.Rn

I. INTRODUCTION

Random matrices (RM) have been investigated intensively in the past decade due to their wide range of applications to different branches of physics such as the theory of mesoscopic fluctuations in disordered conductors [1], spin glass models [2], light propagation in dense media [3], and quantum chaos [4] among others. Random matrices have been useful tools in bringing out universal behavior. It is indeed astonishing that the distributions of energy level spacings of heavy nuclei, the quantum spectra of a Sinai billiard, and the spacing of the zeros of the Riemann ζ function all obey very closely the Wigner surmise. These systems are in the universality class of the Gaussian ensembles (GE), which include the orthogonal, unitary, and symplectic symmetries. As pointed out by Cizeau and Bouchaud [5] (CB), a kind of central limit theorem for matrices is at work which drives all systems with the same underlying symmetries towards a common fixed point behavior. It is natural then to probe the limits of the basin of attraction of Gaussian ensembles. One way to do this is by extending the matrix model to full matrices with strongly fluctuating elements [5]. By strongly fluctuating elements we mean random numbers from a long tailed distribution whose variance and average can diverge. This violates the premises of traditional random matrix theory [6] where the average and variance are finite. CB named such matrices *Lévy matrices* because the generalization is in the same spirit as the broader central limit theorem leading to the universality classes of Lévy [7].

Recently CB studied Lévy matrices, where matrix elements are distributed according to $P(H_{ij})$ with

$$P(H_{ij}) \underset{H_{ij}\to\infty}{\sim} \frac{H_0^{\mu}}{|H_{ij}|^{1+\mu}}, \tag{1}$$

where H_0 is the typical order of magnitude of H_{ij} and the parameter μ ranges from 0 to ∞. The distribution of Eq. (1) has finite variance for $\mu>2$ while the variance diverges for $0<\mu\leqslant 2$. μ only takes positive values since the distribution is not normalizable for $\mu<0$ (unless one redefines the range of H_{ij}). The distribution above serves to probe the limits of the Gaussian universality for full matrices as one changes μ. Based on studies of the distribution of level spacings and the inverse participation ratios of the eigenfunctions, CB found a phase diagram in the μ-energy space showing three regions; for $\mu>2$ they report a regular Gaussian Orthogonal Ensemble (GOE) phase (phase I), i.e., delocalized states and Gaussian orthogonal level spacing distribution. This phase extends to the $1<\mu<2$ interval for a limited range of energies near $E=0$ (which becomes the full band for $\mu\geqslant 2$). Beyond this energy one enters a mixed phase (phase II), showing both localized and extended features, according to two different definitions of the inverse participation ratio [5]. Phases I and II, in the $1<\mu<2$ parameter range, appear in analogy to a mobility edge in disordered metallic systems but, in the ''mixed'' phase, the wave functions presumably decay algebraically. Between $0<\mu<1$, the mixed phase persists up to an energy $E_c(\mu)$ beyond which a third, strictly localized phase (inverse participation ratio finite and Poisson spectra) appears. CB's focus was set on the level spacing distribution as the main spectral signature. Nevertheless the

*Author to whom correspondence should be adreessed. Electronic address: ernesto@pion.ivic.ve

level spacing distribution only reveals very local spectral properties. For example, it is known that while an integrable system has a Poissonian distribution of level spacings its Δ_3 statistic shows rigidity beyond a certain energy scale [8]. A more complete description of the Hamiltonian system involves the studies of longer ranged statistics, such as Δ_3, the level number variance, and the two level correlation function. Also useful, in connection with the wave function structure, is to derive the evolution of the spectra with an abstract ''time'' variable (or perturbation) representing an external field or changes in the boundary conditions. The latter study can reveal quantities such as the ''conductance'' of the system [9,10] and universal features through the distribution of level curvatures and the level velocity autocorrelator [11]. We will then explore the effects of strongly fluctuating matrix elements on the universal features mentioned above.

Lévy matrices are interesting beyond the mere generalization of Gaussian matrices as they can model electronic systems with power-law decaying (with distance) transition elements [12], and spin glasses with dipolar or Ruderman-Kittel-Kasuya-Yosida (RKKY) interactions [5]. Furthermore, Lévy matrices permit interpolation between Gaussian matrices and sparse matrices, showing the corresponding ''percolation'' transition [13], where the matrix disintegrates into separate uncorrelated blocks. Finally, an interesting issue worth noting is the existence of an intermediate ''critical phase,'' between conducting (Gaussian orthogonal/Gaussian unitary ensembles) and insulating phases. Such a phase is of particular interest in connection with the study of spectral distributions at criticality (metal insulator transition). Presumably in this critical regime the wave function decays in an algebraic fashion and one would like to see the spectral signature of such a behavior [14]. The intermediate phase of CB exists over an extended range in values of the parameter μ, making it much simpler to study in principle.

The outline of the paper is as follows. In Sec. II we will study the Lévy matrix density of states by numerically diagonalizing large $N\times N$ matrices. Here we will discuss CB's predictions regarding the sparse matrix limit close to the band center. We will also analyze an extension of the Lévy matrices to show, explicitly, the existence of structures (for finite N) typical of sparse matrix ensembles [15].

In Sec. III we study level statistics and dynamics using 2×2 Lévy matrices of the form

$$\mathcal{H}=\mathcal{H}_S+i\alpha\mathcal{H}_A. \tag{2}$$

The subscripts S and A denote symmetric and antisymmetric Lévy matrices, and α is a symmetry breaking parameter or fictitious time. For the 2×2 model we can solve analytically for small level spacing limit and show that for certain values of μ universal geometrical repulsion is broken. We also find nontrivial decays for the large level curvature tails for $\mu<1$.

In Sec. IV we study level dynamics numerically, for large matrices, using the Hamiltonian of Eq. (2). Taking advantage of the sharp changes of the Δ_3 statistic, we first map the phase diagram drawn qualitatively by CB. The Δ_3 statistic shows unique behavior in the mixed phase, in between logarithmic (GOE) and linear (Poisson) behavior. Following that, we depict the level dynamical character of each of the phases, showing the reduction of sensibility to changes in the boundary conditions as μ decreases (disorder increases). We further characterize the mentioned phases by determining the scaling, with matrix size, of the ''conductance,'' as defined through level curvature. We end with a discussion and conclusions.

II. DENSITY OF STATES AND SPARSE MATRIX LIMIT

Wigner has shown that as long as the average and variance of the matrix elements are finite, the semicircle law for the density of states is approached as $N\to\infty$ [16]. With the Lévy matrix model one explicitly violates the above conditions as matrix elements can have diverging variance and mean. CB have already shown, analytically, that the density of states (DOS) for Lévy matrices assumes the new form

$$\rho(z)=L_\mu^{C(z),\beta(z)}(z), \tag{3}$$

where $L_\mu^{C,\beta}$ is a centered Lévy distribution [7] and C,β are self-consistently determined functions [5]. Such density has an infinite range for z in contrast to the well known Wigner semicircle. Here we are particularly interested in the behavior of Eq. (3) when $\mu\to 0$. CB have argued that, in such a limit, the sparse matrix limit should be achieved. The conclusion is based on the fact that there is a hierarchy of matrix element sizes, the largest of which dominate the spectrum. Very large elements with a finite probability dominate over small ones (which behave effectively as zero) at each column or row defining a sparse matrix. Extensive studies on sparse matrices by Evangelou [15] have shown that the DOS differs from the semicircle by developing a δ-function-like peak with a $1/|E|$ energy dependence at the center of the band (see also [17]). Further singularities show up symmetrically around $E=0$.

Although Eq. (3) predicts a peaked structure in the center of the band as $\mu\to 0$ it does not bear the correct energy dependence for the sparse limit. In fact, as $\mu\to 0^+$, the central maximum has the form $a(\mu)+b(\mu)E^2$ where $a(\mu\to 0)$ diverges. The latter behavior is confirmed by our numerics, showing no sign of the characteristic features of the sparse matrix DOS approaching from $\mu=0^+$.

In order to see the sparse matrix limit we have generalized Lévy matrices to the range $\mu<0$ where random numbers occur in the interval $[-1,1]$ (for normalizability). In a sense, the distribution in this range has long tails towards zero instead of infinity. Although this case conforms to the Wigner theorem, its finite size effects reveal, close to $\mu=0$, the underlying sparse matrix limit.

We generated more than 2000 matrices of up to 1000×1000 and determined the corresponding DOS. Great care was taken of the numerical precision of the code so that small elements were not arbitrarily set to zero. We studied the DOS for various matrix sizes to check for the asymptotic behavior. In Fig. 1 we show a phase diagram for the DOS as a function of the parameter μ, for both negative and positive values. In the positive μ regime, we confirm CB's results; as depicted in the figure, the DOS approaches the semicircle for $\mu>2$ while for $0<\mu<2$ it reaches a new stable form as a function of the matrix size N. For $\mu<0$ (tails towards zero),

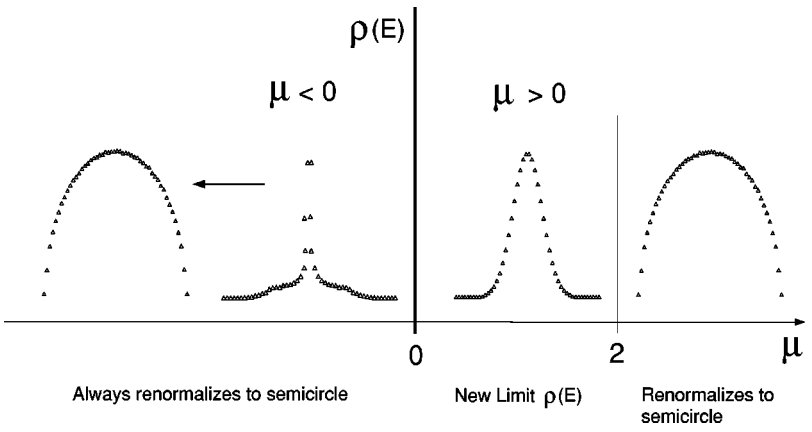

FIG. 1. Phase diagram for the density of states as a function of the parameter μ. On the right-hand side we show the Gaussian phase converging to the semicircle and CB's new limit DOS for $0<\mu<2$. On the left, i.e., $\mu<0$, the limit DOS is always the semicircle but, for finite size matrices one observes a sharp singularity developing with a $1/|E|$ energy dependence characteristic of sparse matrix ensembles. Additional subsidiary anomalies begin to develop on both sides of the DOS maximum.

if one fixes the matrix size, there are two regimes as a function of μ; for $|\mu|$ sufficiently large the DOS follows the semicircle while for $\mu\to 0^-$, $\rho(E)$ crosses over to a new form and starts to develop a sharp singularity of the form $1/|E|$ when $|E|\to 0$. Additional singularities develop around $|E|=1$ as expected for sparse matrices. Obviously, for any $\mu<0$ the DOS renormalizes towards the semicircle law when $N\to\infty$. Therefore, the sparse matrix behavior is only a finite size effect *except for* $\mu=0$, where the sparse matrix limit is asymptotic.

In order to see the asymptotic form for $\rho(E,\mu=0)$, one has to scale out the N dependence. As the matrix size N increases, one needs to lower $|\mu|$ in order to preserve the shape of the density. Using the nontrivial scaling variable μ/N^{γ} with $\gamma=0.83\pm 0.02$, we obtain an invariant form for the DOS reflecting the limit behavior at $\mu=0$ (see Fig. 2). The scale factor also tells us how the semicircle is approached as N increases. On the $\mu>0$ side, small matrices never exhibit sparse-matrix-like behavior, indicating that the analytical form of the DOS changes discontinuously at $\mu=0$. We have not found a simple explanation for the value of the exponent γ.

III. LEVEL SPACING AND CURVATURES IN THE 2×2 MODEL

The study of 2×2 model matrices is useful in obtaining approximate features of the local spectral behavior of large matrices. A prominent example is the Wigner surmise; while only rigorous for 2×2 matrices, it reproduces remarkably well large N features (for Gaussian disorder). The small level spacing behavior is expected to be well reproduced by an $N=2$ theory because a very close encounter of two levels is weakly affected by the rest. By the same argument, the tails of the level curvature distribution should also be well reproduced as close encounters involve the largest curvatures. The previous argument is especially clear within the level dynamical picture, where levels interact via an inverse square potential of their separation [18].

Regarding the 2×2 model when an external flux is applied; up to the correlation flux ϕ_c (defined below) levels should evolve parabolically without crossing other levels. Beyond such a flux, level collisions typically start [19], and the $N=2$ model should cease to be valid. The shortcomings of the 2×2 model for larger spacing (smaller curvature) can be in part circumvented by adding a thermal reservoir representing the other levels. We do not pursue the latter approach but refer the reader to Ref. [20] where it is discussed in detail.

We will be especially interested in the universal property of *geometrical repulsion.* Geometrical means that repulsion is due to the Jacobian which relates volume elements in the matrix and eigenvalue spaces. Such behavior is obviously well reproduced by the 2×2 model. We will find that in certain ranges of the parameter μ such universality is broken. Nevertheless, we emphasize that in this section we use the *full Lévy distributions* instead of only their characteristic tails as in the preceding section. Such a choice is central to the geometrical breaking phenomenon because it depends on essential singularities of the Lévy distribution for small arguments.

We study the level dynamics in response to a perturbation by using the model of Eq. (2). Dupuis and Montambaux [21] have argued that α, in this model, plays a role similar to the phase in an Aharonov-Bohm ring, the mapping being

$$\alpha=\sqrt{\frac{\pi E_c}{N\Delta}}\phi, \tag{4}$$

where ϕ is defined by $\Psi(2\pi)=\Psi(0)\exp(i\phi)$ acting as a change in the ''boundary conditions'' to which the response in the energy levels can be measured. E_c is the Thouless

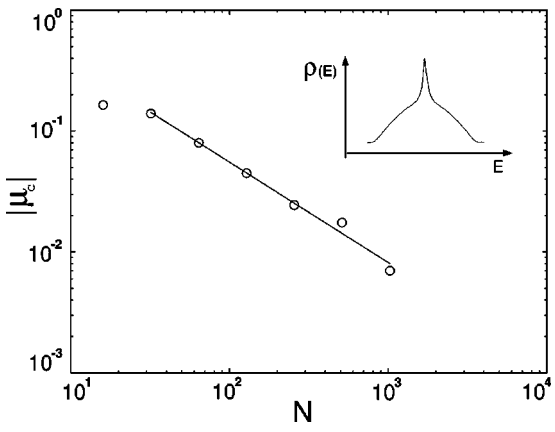

FIG. 2. Scaling of $\rho(E)$ for $\mu<0$ in order to bring about the sparse matrix limit as $\mu\to 0^-$. As N increases μ is reduced to preserve the shape of the density (inset). The sparse matrix limit is achieved only in the $\mu=0$ limit.

correlation energy and Δ is the mean level spacing. Then the correlation flux is $\phi_c=\sqrt{N\Delta/(\pi E_c)}$ setting $\alpha=1$ and attaining the unitary limit.

First, we will look at the small level spacings in the cases $\alpha=0$ or orthogonal and $\alpha=1$ or unitary limits. Consider the matrix

$$\begin{pmatrix} x_1+x_2 & x_3+i\alpha x_4 \\ x_3-i\alpha x_4 & x_1-x_2 \end{pmatrix}, \tag{5}$$

where x_i are real random numbers taken from a symmetric (or symmetrized) Lévy distribution $L_{\mu,\beta=0}$. The parameter μ is the same as that defined in Eq. (1) describing the distribution tails. β is an asymmetry parameter which is set to zero throughout. We have chosen to work directly with a Lévy stable function instead of using CB's function with power-law tails. This choice has important consequences regarding the local spectral behavior because of the peculiar dependence of $L_{\mu<1,\beta=0}(x)$ for small x values. We show below that the behavior of the large value tails of the matrix elements cannot affect the universality of the small level spacing behavior. For further details on Lévy distributions, we refer the reader to an excellent review by Bouchaud and Georges [7].

The spectrum of the Hamiltonian above is given by

$$E_{\pm}=x_1\pm\sqrt{x_2^2+x_3^2+\alpha^2x_4^2} \tag{6}$$

and the energy spacing $E_+-E_-=s(\alpha)=2\sqrt{x_2^2+x_3^2+\alpha^2x_4^2}$. The distribution function of s is given by

$$P_\alpha(s)=\int \delta(s-2\sqrt{x_2^2+x_3^2+\alpha^2x_4^2})\prod_{i=1}^{4} P(x_i)dx_i. \tag{7}$$

As can be seen from the expressions above, small values of s will result from small simultaneous values of x_i.

1<μ<2 range

Small x_i yield small s values, so we use the following expansion:

$$L_{\mu,0}(x\to 0)=\frac{1}{\pi\mu}\sum_{k=0}^{\infty}(-1)^k\frac{x^{2k}}{2k!}\Gamma\left(\frac{2k+1}{\mu}\right), \tag{8}$$

valid for small x [7]. The radius of convergence of Eq. (8) is infinite for $1<\mu<2$. Performing the integrals in Eq. (7) we arrived at the expressions, for $s\to 0$,

$$P_\alpha(s,1<\mu<2)=\begin{cases}\dfrac{\Gamma(1/\mu)^3}{128\pi^2\mu^3}s^2 & \text{if } \alpha=1,\\[2ex] \dfrac{\Gamma(1/\mu)^2}{8\pi\mu^2}s & \text{if } \alpha=0.\end{cases} \tag{9}$$

We thus confirm the universal level spacing behavior given by the first power of the spacing s, in the orthogonal case, and a second power in the unitary case. *The level repulsion is geometrical*. The borderline case $\mu=1$, i.e., the Cauchy distribution for matrix elements, can be computed exactly obeying the expression

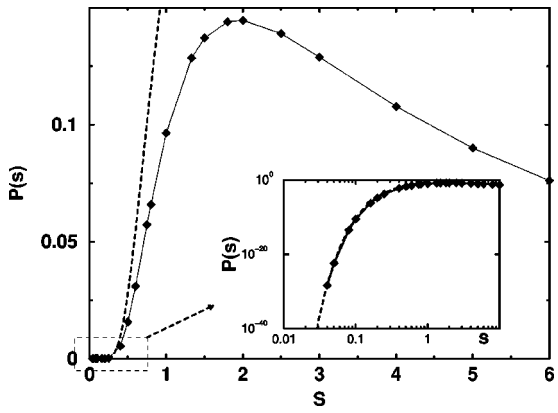

FIG. 3. Level spacing distribution for the 2×2 model and $\mu=1/2$. The full distribution (solid line) was obtained numerically. The analytic expression for the $s\to 0$ limit (dashed line) is shown to fit the numerical solution in the inset. Geometrical repulsion is then broken.

$$P_\alpha(s,\mu=1)=\mathrm{Re}\left[\frac{16s\tanh^{-1}(\sqrt{4+s^2}/2)}{\sqrt{4+s^2}\pi^2(s^2+8)}\right]. \tag{10}$$

The expansion for small spacings is $(\ln 4-\ln s)s/\pi^2$. Therefore, for the $\mu=1$ case, repulsion is nontrivial. Such behavior reflects on the curvature distribution.

0<μ<1 range

In this range the Lévy functions are generally integral expressions and we do not know of simple asymptotic expressions for small arguments. Therefore, we have chosen to solve for particularly simple cases which include $\mu=1/2$ and $\mu=1/3$ within the mixed phase and outside the range of validity of the expansion of Eq. (8). The Lévy distribution for $\mu=1/2$ is simply

$$L_{1/2,0}(x)=\frac{C}{\sqrt{2\pi}x^{3/2}}\exp(-C^2/2x), \tag{11}$$

where C is a normalization constant. Using Eq. (11) we can obtain, after numerical integration, the distribution depicted in Fig. 3. The behavior of small spacings is obviously nonlinear. The universal geometrical repulsion is thus broken for the orthogonal and unitary cases when $0<\mu<1$.

We can also expand the corresponding integral for small energy spacings obtaining the expression, for $s\to 0$,

$$P_\alpha(s,\mu=1/2)=\frac{16}{3}\frac{(2+\alpha^{2/3})^{3/4}\exp[-(2+\alpha^{2/3})^{3/2}/s]}{s^{3/2}\pi}. \tag{12}$$

Note that the small spacing behavior (the power of s) is not sensitive to the change of symmetry (given by α). Furthermore, Eq. (12) shows the same behavior for small arguments as Eq. (11), with $\mu=1/2$ and $C=\sqrt{2}(2+\alpha^{2/3})^{3/4}$. This says that the initial Lévy distribution gets its parameter C renormalized under the variable combination $\sqrt{x_2^2+x_3^2+x_4^2}$, but the form of the distribution remains unchanged. Using the hypothesis that in the range $0<\mu<1$ the form of the Lévy distribution governs the small level spacing behavior, we conjecture that the function of μ is of the form, for $s\to 0$,

$$P_\alpha(s,0<\mu<1)=\frac{f(\mu,\alpha)}{s^{(2-\mu)/2(1-\mu)}}\exp\left(-\frac{g(\mu,\alpha)}{s^{\mu/(1-\mu)}}\right), \tag{13}$$

where the general forms of f and g have not been determined. We have checked this general conjecture for the value $\mu=1/3$; $L_{1/3}(x)=(u/\pi)\sin(\pi/3)K_{1/3}(u/x^{1/2})/x^{3/2}$ where $K_{1/3}$ is the modified Bessel function of order 1/3 and u is a constant. In the limit $\mu\to 0$ Eq. (13) implies $P(s)\to 1/s$ and level repulsion turns to a nontrivial level clustering with a divergence at zero spacing. Equation (13) is undetermined for $\mu=1$. It is apparent that, at least within the 2×2 matrix model, the repulsion *ceases to be geometrical* and a new μ dependent level statistical phase takes over. Such behavior is due to the essential singularity of $L_{\mu<1}(x)$ for small arguments. If one uses a reasonably behaved $P(x)$ at small x preserving power-law tails (appropriately normalized), geometrical repulsion is the rule. From this analysis, it is apparent that the tails of the distribution do not induce any special local spectral behavior. Notwithstanding, the long ranged spectral rigidity is influenced by the long tails, giving a new Δ_3 signature discussed in Sec. IV. We will discuss in the last section similar nongeometrical repulsion in the context of the Dyson plasma picture in a weak power-law potential.

Level curvatures

The tails of the probability distribution of level curvatures have been shown to be universal [22]. Therefore, changes in their behavior should signal changes in the universality class. The universality of curvature tails is known to be closely related to that of small level spacing distribution. This is intuitive by the argument that largest curvatures occur on the closest encounters between energy levels.

For the 2×2 model the level curvature is defined as

$$\kappa(\alpha)\equiv\frac{\partial^2 s(\alpha)}{\partial\alpha^2}=\left\langle\frac{2x_4^2}{s(\alpha)}-\frac{8\alpha^2x_4^4}{s^3(\alpha)}\right\rangle, \tag{14}$$

where $s(\alpha)$ is the level spacing. The distribution of curvatures is then computed by using an equation analogous to Eq. (7). For large curvatures it is expected that the many level interaction becomes negligible and the 2×2 approximation is very good [23]. Moreover, as we will see, in the limit $\mu\to 0$ repulsion is very weak compared to the large energies involved, so the 2×2 matrix is again justified.

For $\mu=2$ the Lévy distribution corresponds to a Gaussian. This case was studied extensively by Kamenev and Braun [19]. For $\alpha=0$ the large κ behavior corresponds to $P_\alpha(\kappa)\sim\kappa^{-3}$. On the other hand, the behavior changes when $\alpha=1$ (unitary case) where $P_\alpha(\kappa)\sim c\exp(-8\kappa^2/2)$. Such deviation from universal behavior (as κ^{-4}) is related to the breakdown of the 2×2 model as $\alpha\to 1$. For further discussion on this point see Ref. [19]. κ^{-3} behavior is also obtained if one uses a distribution with a well behaved bulk (no essential singularities for small matrix elements) and a tail decaying as $1/x^{\mu+1}$ with $\mu>1$. Gaussian universality in the regime $1<\mu\leqslant 2$ for the level spacing, found previously, also suggests a well behaved curvature distribution in this range.

In the range $0<\mu\leqslant 1$ we have studied three cases, i.e., $\mu=1/3$, 1/2, 1 as with the level spacing distribution. Using a relation analogous to Eq. (7) we were only able to obtain the level curvature tail behavior, in the limit $\alpha\to 0$. Fortunately, this is the limit where the 2×2 model emulates well the large N results [19] relevant to physical systems. Our results are summarized as follows:

$$\mathcal{P}(\kappa)\sim\begin{cases}1/\kappa^{5/3} & \text{for } \mu=1/3,\\ 1/\kappa^{5/4} & \text{for } \mu=1/2,\\ 1/\kappa^{3/2} & \text{for } \mu=1.\end{cases} \tag{15}$$

As with the level spacing, the power of the curvature tail varies continuously with μ in the mixed phase in a nontrivial fashion. The first two results can be derived analytically expanding for large κ values. On the other hand, for $\mu=1$ we obtained the joint probability distribution for (κ,s),

$$\mathcal{P}(\kappa,s)=\mathrm{Re}\left[\frac{32s^{3/2}\tanh^{-1}(\sqrt{4+s^2}/2)}{\pi^2\sqrt{\kappa}\sqrt{4+s^2}(4+\kappa s)(8+s^2)}\right]. \tag{16}$$

We were not able to obtain a closed expression integrating over s. Nevertheless, if one takes the $s\to 0$ first and then the limit $\kappa\to\infty$ we obtain the result predicted by Eq. (15). An alternative procedure is to obtain the distribution by introducing Cauchy random variables into Eq. (14) and sampling the κ values. This procedure showed a clear asymptotic dependence as $1/\kappa^{3/2}$ in consistency with the previous order of limits.

As pointed out in the beginning of this section, if we use an only tails version of the Lévy distributions, geometrical repulsion and curvature tail universality are preserved. We have tested this explicitly with the distribution $\mu/(x+1)^{\mu+1}$, which has regular behavior at small values for all μ.

IV. LEVEL STATISTICS AND DYNAMICS OF LARGE MATRICES

We will now concentrate on the level statistics and dynamics of large matrices whose matrix elements come from Eq. (1). CB probed the level spacing distribution, the DOS, and the wave function, the latter through two definitions of the inverse participation ratio. Useful information can be retrieved from level dynamics regarding the ''conductance'' of the matrix model. This is possible due to the very general definition of conductance in terms of level sensibility to changes in the boundary conditions [24]. Such sensibility is quantified through the computation of level curvatures with respect to the parameter α in Eq. (4). Furthermore, we will analyze the Δ_3 statistic which is suited to the study of inhomogeneous spectra, probing longer ranged behavior than level spacing distributions.

In order to corroborate the phase boundaries proposed by CB we have calculated the Δ_3 statistic which gives very sharp changes in behavior as a function of the energy interval around the band center. The Δ_3 statistic is computed using the following expression:

$$\Delta_3(L)=\left\langle\frac{1}{L}\min_{A,B}\int_{-L}^{L}[N(\epsilon)-A\epsilon-B]^2d\epsilon\right\rangle, \tag{17}$$

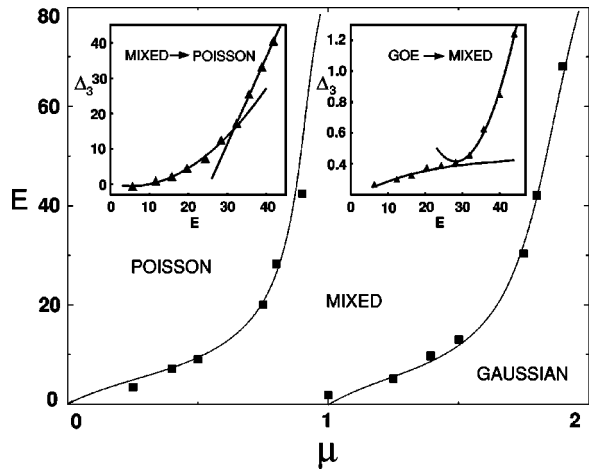

FIG. 4. Phase boundaries using the Δ_3 statistic between the Gaussian, mixed, and Poisson phases as a function of the energy (dimensionless) and μ. For $1<\mu<2$, the inset shows the rapid crossover between logarithmic (Gaussian) and quadratic (mixed) behavior. For $0<\mu<1$, the inset shows the crossover between quadratic (mixed) and linear (Poisson) behavior. Fits are shown to logarithmic and quadratic behaviors. The mapping of the phase boundaries as a function of μ is possible due to the sharp changes of the Δ_3 statistic.

where $N(E)$ is the number of levels with energies between 0 and E. The energy interval varies between $[-L,L]$. It is well known that Gaussian statistics imply a logarithmic Δ_3 function for both orthogonal and unitary ensembles. On the other hand, Poisson statistics imply a linear behavior. Figure 4 (insets) shows both the transition from Gaussian to mixed phase statistics, and from the latter to Poisson. We find that Δ_3 behaves quadratically with energy for the mixed phase, giving it a characteristic signature. Departure from logarithmic behavior indicates a relaxation of the long ranged spectral rigidity of the Gaussian ensembles. The changes in Δ_3 from one range to another are so sharp that one can use it to map the range boundaries as a function of μ. Figure 4 shows the approximate phase diagram obtained from this exercise, confirming the qualitative behavior proposed by CB.

We now study the level dynamics using the Hamiltonian of Eq. (2) and matrix element distribution given by Eq. (1). We have diagonalized matrices of up to 1000×1000 and drawn the eigenvalues as a function of the abstract time parameter α. Figure 5 shows typical ''spaghetti'' for each of the phases found by CB. The Gaussian of the spectrum is seen to expand due to increased repulsion of the energy levels [as we go to the Gaussian unitary ensemble (GUE) limit] as a function of α. Sufficiently large values of α eventually give all eigenvalues a linear dependence [20].

As one goes from the Gaussian phase (center of band) into the mixed phase [Fig. 5(a)], one sees ''solitons'' developing at the edge of the spectrum. The soliton, propagating

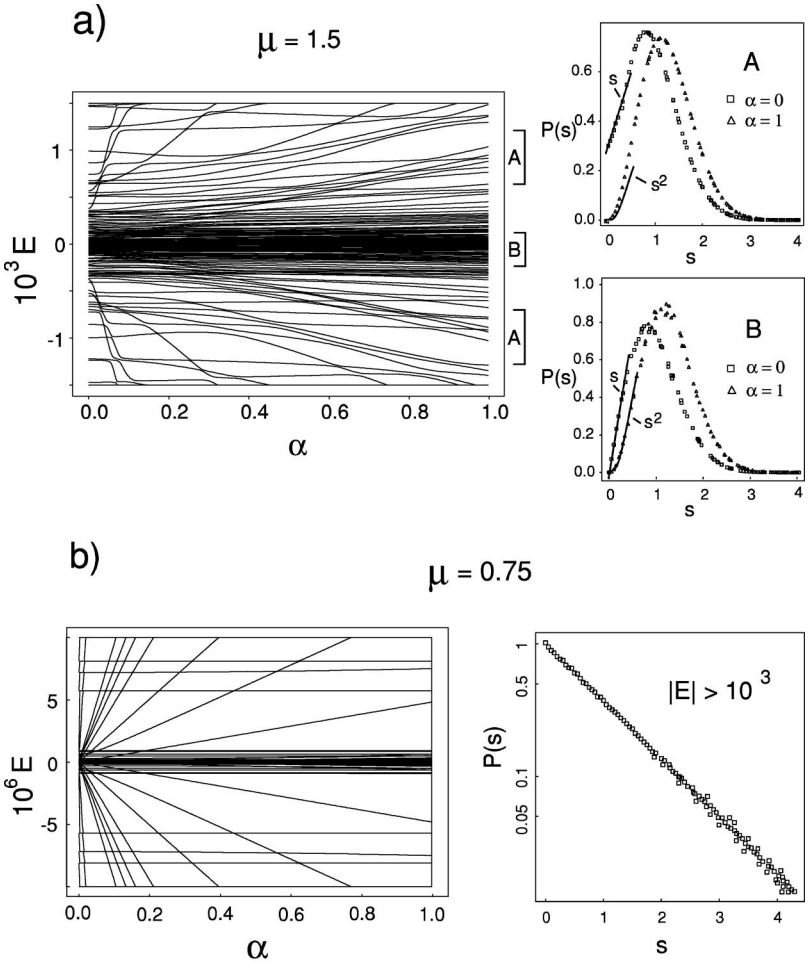

FIG. 5. In the figure we show the character of level dynamics (energy versus α) in each of the CB phases as discussed in the main text. (a) The left shows the mixed and Gaussian energy ranges labeled *A* and *B*, respectively. On the right we show the corresponding level spacing distributions. (b) The left shows the mixed and Poisson energy ranges. On the right, the exponential level spacing distribution for the Poisson regime. The energy E is dimensionless.

without change in form in the abstract time parameter, consists of a set of levels with persistent slopes (known as persistent level crossing). Such a behavior is not seen in regular random matrix ensembles. Nevertheless, simple matrix models have been suggested in the past [18] that show similar behavior. This persistent behavior is reminiscent, as pointed out by Nakamura [18], of scarred states occurring very commonly in the spectra of a quantum stadium billiard [25]. Scarred states are due to unstable periodic orbits because of, for example, bouncing between plane parallel walls of the stadium. In a similar fashion, the persistent level velocities in the mixed phase occur due to large off diagonal elements connecting two states, producing a periodic ''bouncing.'' This agrees with CB reasoning that a quasieigenvector at these energies has the form $1/\sqrt{2}(|i\rangle+|j\rangle)$ because of a very large matrix element H_{ij}.

Regarding the level spacing distribution [see Fig. 5(a)] for $1<\mu<2$ we see geometrical repulsion, i.e., s and s^2 dependences for small s. Nevertheless, the large spacing behavior varies with energy from a Gaussian decay (as in GOE), to closer to an exponential decay in CB's mixed phase. The mixed phase retains geometrical level repulsion, as shown in Fig. 5(a), but the distribution departs from a finite value at spacing zero. This could indicate that we have a mixture of Gaussian- and Poisson-like behavior, i.e., a set of localized states in coexistence with extended states. Mixture of statistics has been observed for critical disorder in tight binding random matrices [26] (see also Ref. [14]).

Reducing the parameter μ below 1 [Fig. 5(b)], we enter the new regime of CB's diagram where, depending on energy, one is within the mixed phase (center of the band) or in the strictly localized regime (edges of the band). The mixed phase (center of the band) in Fig. 5(b) is very compressed, nevertheless it shows the same character of the edge of the band in Fig. 5(a). In the Poisson phase, the spectrum literally explodes in solitonic or persistent level behavior. As can be seen in Fig. 5(b), the spectrum at the edge of the band is made from horizontal levels directly reflecting large elements from the symmetric part of the Hamiltonian. The linearly increasing levels reflect large dominant elements from the antisymmetric contribution. Horizontal levels show the insensibility to changes in the boundary conditions (α) and thus localization. In the mixed phase there is a remnant curvature, seen in the border of the band in Fig. 5(a), possibly signaling what CB identified as algebraic decay of the wave functions. Such features are not seen in the center of the band in Fig. 5(b) (same phase) because of the scales.

Finally, for $0<\mu<1$ higher in energy, the spacing distribution becomes Poisson as seen in the right-hand panel of Fig. 5(b). With the exception of the very center of the band, all levels are either horizontal or lines of a fixed slope [Fig. 5(b)]. The matrix can be thought to break up into weakly coupled 2×2 blocks. Different levels only ''see'' each other on very close encounters (barely visible in the figure), at which point they avoid crossing.

As mentioned in the Introduction, there is a very general definition of ''conductance'' of a physical system based on the sensitivity of a block of material to changes in the boundary conditions. In our case, boundary conditions are changed by the parameter α. The Thouless definition for the conductance is abstract enough to encompass any model where one

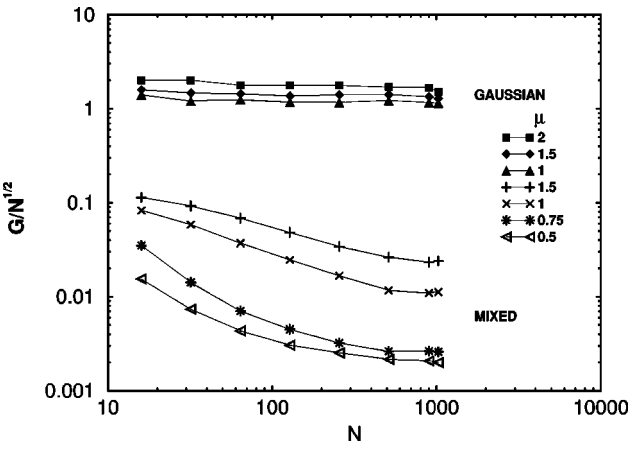

FIG. 6. The conductance scaled by $\sqrt{N}$ as computed from Eq. (18) for each of the three phases. While conductance in the Gaussian region grows as $\sqrt{N}$, in the mixed phase the conductance has an additional, presumably logarithmic decrease, indicating very weak localization. The averages indicated in Eq. (18) are performed within the corresponding energy ranges.

can produce the spectrum and the effects of a coupled external parameter. In our case, the spectrum is inhomogeneous so the Thouless conductance must be computed within restricted energy ranges. The Thouless formula [27] for the conductance used here is

$$G=\frac{1}{\Delta}\left\langle\left(\frac{d^2E}{d\phi^2}\right)^2_{\phi=0}\right\rangle^{1/2}, \tag{18}$$

where Δ is the average level spacing computed within each phase. Different conduction regimes are usually distinguished by their scaling properties with system size. Previous studies with banded random matrices [28], where a scaling parameter associated with ''length'' can be defined, have shown both the metallic and localized regimes. In the latter case, banded matrices show Ohmic conductance behavior of one-dimensional systems scaling as $1/L$ and localized behavior scaling as $\exp(-L)$, where L is identified with N the matrix size.

In our case there is no clear length parameter and the system size is governed by the matrix dimension N. The metallic regime should show an increasing conductance with matrix size going as $\sqrt{N}$. Such a behavior is expected in the Gaussian regime, as found analytically by Simons and Altshuler [11,29] and shown numerically by Sano [30] for the quantum kicked rotator in the chaotic regime. We take the latter N dependence as reference to contrast with the behavior of the mixed phase.

Using the spectra as a function of α we have computed the conductance according to Eq. (18), averaged within each of the phases described in Fig. 4. The scaled conductance as a function of matrix size is depicted in Fig. 6. Within the Gaussian regime we see that $G/\sqrt{N}$ is relatively constant, confirming the theoretical result. The magnitude of the conductance also gets reduced as disorder increases (μ decreases) as expected.

For the mixed phase we see an appreciable decrease in $G/\sqrt{N}$ as N increases. Nevertheless, the decrease is slower

than algebraic, as can be seen from Fig. 6. The mixed phase then has an additional weakly localized contribution as compared to the Gaussian phase. Such behavior is in accord with the algebraic decay of the wave functions where electrons have no length scale for localization. Finally, for the Poisson phase we found extremely small conductances, zero within the numerical error. As expected, levels do not respond to α in this (μ,E) range.

V. DISCUSSION AND CONCLUSIONS

We have presented a spectral study of Lévy matrices which significantly extends results found by Cizeau and Bouchaud [5]. We have shown, by generalizing the Lévy matrix model to $\mu<0$, how the sparse matrix limit is reached as $\mu\to 0$. $\mu=0$ is an unstable fixed point in the renormalization group sense, $\mu=0^-$ leading to the Wigner semicircle fixed point and $\mu=0^+$ to a new CB fixed point as the matrix size N increases.

We solved 2×2 matrix models analytically to check whether geometrical repulsion, a trademark of the Gaussian ensembles, is broken in Lévy matrices. The 2×2 model is justified especially for $\mu<1$ where the close encounter of two levels is weakly affected by the rest of the spectrum. We found that, unexpectedly, the long tails of the distribution (for $\mu>0$) do not affect geometrical repulsion. Nevertheless, essential singularities of $L_{\mu<1}(x\to 0)$ break geometrical repulsion, making it μ dependent, i.e., nonuniversal. A strong nonlinear repulsion remains for which we have found a general form. Only for $\mu=0$ is repulsion replaced by strong level clustering as $P(s\to 0)\sim 1/s$.

Our study of large $N\times N$ Lévy matrices focused on both spectral statistics and dynamics. We found that the Δ_3 statistic exhibits very sharp crossovers between the surmised phases of CB. We used this characteristic to map the phase boundaries as a function of μ and energy as discussed in Sec. IV. The Δ_3 statistic, measuring longer ranged statistics than the level spacing, has a new quadratic dependence for the mixed phase. Notwithstanding, level repulsion is geometrical except for the fact that it departs from a finite value at spacing zero. Regarding level dynamics, we have obtained a clear picture of how the system goes from the eigenstate extended Gaussian phase to the localized Poisson phase. For $\mu>2$ the whole band obeys $1/\kappa^3$ curvature tails as expected. Decreasing μ below 2 begins to develop solitoniclike structures at the band edges. The interpretation of this is that clusters of states become localized, and we have periodic bouncing between such states in the same way scars appear on the stadium billiard. Below $\mu=1$ solitonic structures dominate the spectrum with the exception of the center of the band. Away from the center, in this regime, one starts to see levels completely insensible to the fictitious time parameter α. The only curvature they exhibit is on very short ranged encounters with a radiating level.

Motivated by the work of Casati *et al.* [28] we studied the scaling properties of the ''conductance'' as a function of matrix size. While the Gaussian regime exhibits a conductance proportional to $\sqrt{N}$ as expected from theory, we found that the mixed phase has an additional, slower than algebraic, decrease. CB had found power-law decaying eigenfunctions indicating a special kind of broad metal insulator transition region.

Finally, we note an interesting connection to a recent model involving Dyson's plasma picture of eigenvalues confined by a potential. Canali [31] proposed the latter potential to be extremely weak, considering either $V(\epsilon)=A/2|\epsilon|^{\nu}$ with $0<\nu<1$ or $A/2\ln^2|\epsilon|$, both as $\epsilon\to\infty$. Such a potential presumably produces critical level statistics, as in the metal insulator transition, for a certain value A_c. Curiously he finds a peaked DOS with a $1/|\epsilon|^{1-\nu}$ near the band center. Such behavior is reminiscent of the findings of CB. Furthermore, for the power-law potential the *geometrical repulsion is broken* as in our 2×2 model for Lévy matrices.

It is intuitive that a sufficiently weak confinement potential could yield a very broad band of eigenvalues as we find for the mixed phase. Such a phase is also some kind of wide critical region separating a metallic and a localized phase as Canali's model attempts to describe. A possible relation between the Lévy matrix model and Canali's weakly confined plasma would be illuminating, especially in connection with the level statistics at the Anderson transition.

ACKNOWLEDGMENTS

This project was funded by CONICIT under Grant No. S1-97000368 and the POLAR foundation. E.M. thanks E. Mucciolo for a useful discussion. M.A. thanks PDVSA Intevep for permission to publish this paper.

[1] K. A. Muttalib, J. L. Pichard, and A. D. Stone, Phys. Rev. Lett. **59**, 2475 (1987).
[2] M. Mezard and G. Parisi, Europhys. Lett. **3**, 1067 (1987).
[3] E. Akkermans and R. Maynard, J. Phys. (France) **46**, L1045 (1985).
[4] M. V. Berry, *Quantum Chaos and Statistical Nuclear Physics*, edited by T. Seligman and N. Nishioka, Lecture Notes in Physics Vol. 203 (Springer, Berlin, 1986), and references therein.
[5] P. Cizeau and J. P. Bouchaud, Phys. Rev. E **50**, 1810 (1994).
[6] M. L. Mehta, *Random Matrices and the Statistical Theory of Statistical Levels* (Academic Press, New York, 1991).
[7] J. P. Bouchaud and A. Georges, Phys. Rep. **195**, 127 (1990).
[8] G. Casati, B. V. Chirikov, and I. Guarneri, Phys. Rev. Lett. **54**, 1350 (1985).
[9] E. Akkermans and G. Montambaux, Phys. Rev. Lett. **68**, 642 (1992).
[10] C. M. Canali, C. Basu, W. Stephan, and V. E. Kravtsov, Phys. Rev. B **54**, 1431 (1996).
[11] B. D. Simons and B. L. Altshuler, Phys. Rev. B **48**, 5422 (1993).
[12] L. S. Levitov, Europhys. Lett. **9**, 83 (1989).
[13] V. Ambegaokar, B. I. Halperin, and J. S. Langer, Phys. Rev. B **4**, 2612 (1971).
[14] This issue has been the subject of debate in the literature, see,

for example, B. I. Shklovskii *et al.*, Phys. Rev. B **47**, 11 487 (1993); E. Hofstetter and M. Schreiber, *ibid.* **49**, 14 726 (1994); I. Kh. Zharekeshev and B. Kramer, *ibid.* **51**, 17 239 (1995); A. G. Aronov, V. E. Kravtsov, and I. V. Lerner, Phys. Rev. Lett. **74**, 1174 (1995).

[15] S. N. Evangelou and E. N. Economou, Phys. Rev. Lett. **68**, 361 (1992); S. N. Evangelou, J. Stat. Phys. **69**, 361 (1992).

[16] E. P. Wigner, Ann. Math. **62**, 548 (1955); **65**, 203 (1957).

[17] S. Kirkpatrick and T. P. Eggarter, Phys. Rev. B **6**, 3598 (1972).

[18] K. Nakamura, *Quantum Chaos: A New Paradigm of Nonlinear Dynamics*. Cambridge Nonlinear Science Series 3, edited by B. Chirikov *et al.* (Cambridge University Press, Cambridge, England, 1994).

[19] A. Kamenev and D. Braun, J. Phys. I **4**, 1049 (1994).

[20] J. Zakrzewski and D. Delande, Phys. Rev. E **47**, 1650 (1993).

[21] N. Dupuis and G. Montambaux, Phys. Rev. B **43**, 14 390 (1991).

[22] P. Gaspard, S. A. Rice, H. J. Mikeska, and K. Nakamura, Phys. Rev. A **42**, 4015 (1990).

[23] J. Zakrzewski and M. Kus, Phys. Rev. Lett. **67**, 2749 (1991).

[24] D. J. Thouless, Phys. Rev. Lett. **39**, 1167 (1977).

[25] T. Takami and H. Hasegawa, Phys. Rev. Lett. **68**, 419 (1992).

[26] E. Hofstetter and M. Schreiber, Phys. Rev. B **48**, 16 979 (1993).

[27] J. T. Edwards and D. Thouless, J. Phys. C **5**, 807 (1971); D. Thouless, Phys. Rep. **13**, 93 (1974).

[28] G. Casati, I. Guarneri, F. Izrailev, L. Molinari, and K. Zyczkowski, Phys. Rev. Lett. **72**, 2697 (1994).

[29] E. Mucciolo (private communication).

[30] M. M. Sano, Phys. Rev. E **54**, 3591 (1996).

[31] C. M. Canali, Phys. Rev. B **53**, 3713 (1996).